

# Lawrence Berkeley National Laboratory

LBL Publications

## Title

Structured photocathodes for improved high-energy x-ray efficiency in streak cameras

## Permalink

<https://escholarship.org/uc/item/3zp874xp>

## Journal

Review of Scientific Instruments, 87(11)

## ISSN

0034-6748

## Authors

Opachich, YP

Bell, PM

Bradley, DK

et al.

## Publication Date

2016-11-01

## DOI

10.1063/1.4961302

Peer reviewed

## Structured photocathodes for improved high-energy x-ray efficiency in streak cameras

Y. P. Opachich, P. M. Bell, D. K. Bradley, N. Chen, J. Feng, A. Gopal, B. Hatch, T. J. Hilsabeck, E. Huffman, J. A. Koch, O. L. Landen, A. G. MacPhee, S. R. Nagel, and S. Udin

Citation: [Review of Scientific Instruments](#) **87**, 11E331 (2016); doi: 10.1063/1.4961302

View online: <http://dx.doi.org/10.1063/1.4961302>

View Table of Contents: <http://scitation.aip.org/content/aip/journal/rsi/87/11?ver=pdfcov>

Published by the [AIP Publishing](#)

---

### Articles you may be interested in

[Temporal resolution limit estimation of x-ray streak cameras using a CsI photocathode](#)

J. Appl. Phys. **118**, 083105 (2015); 10.1063/1.4928675

[An x-ray streak camera with high spatio-temporal resolution](#)

Appl. Phys. Lett. **91**, 134102 (2007); 10.1063/1.2793191

[Characterization of CsI photocathodes at grazing incidence for use in a unit quantum efficiency x-ray streak camera](#)

Rev. Sci. Instrum. **75**, 3131 (2004); 10.1063/1.1790558

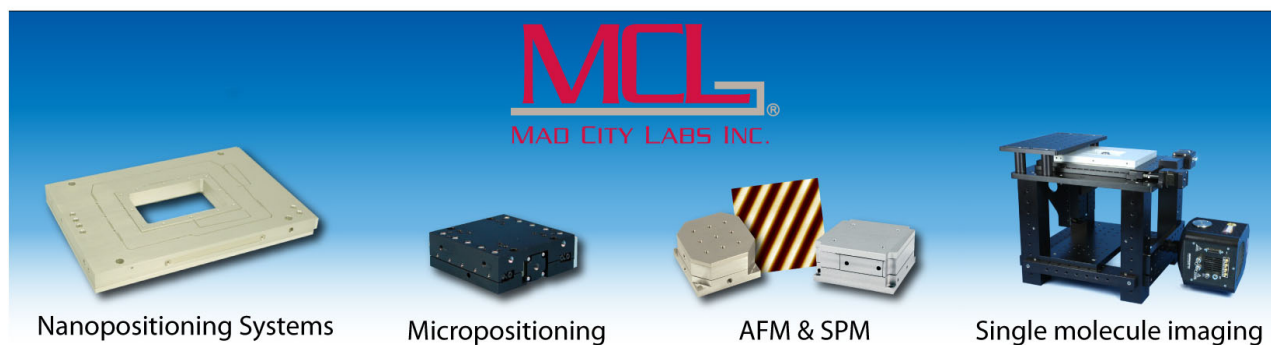
[Optical and x-ray streak camera gain measurements](#)

Rev. Sci. Instrum. **75**, 3956 (2004); 10.1063/1.1787929

[Improvements in off-center focusing in an x-ray streak camera](#)

Rev. Sci. Instrum. **74**, 2245 (2003); 10.1063/1.1538331

---



# Structured photocathodes for improved high-energy x-ray efficiency in streak cameras

Y. P. Opachich,<sup>1,a)</sup> P. M. Bell,<sup>2</sup> D. K. Bradley,<sup>2</sup> N. Chen,<sup>3</sup> J. Feng,<sup>4</sup> A. Gopal,<sup>3</sup> B. Hatch,<sup>2</sup> T. J. Hillsabeck,<sup>5</sup> E. Huffman,<sup>1</sup> J. A. Koch,<sup>1</sup> O. L. Landen,<sup>2</sup> A. G. MacPhee,<sup>2</sup> S. R. Nagel,<sup>2</sup> and S. Udin<sup>3</sup>

<sup>1</sup>National Security Technologies, LLC, Livermore, California 94551, USA

<sup>2</sup>Lawrence Livermore National Laboratory, Livermore, California 94551, USA

<sup>3</sup>Nanoshift LLC, Emeryville, California 94608, USA

<sup>4</sup>Lawrence Berkeley National Laboratory, Berkeley, California 94720, USA

<sup>5</sup>General Atomics, San Diego, California 92121, USA

(Presented 8 June 2016; received 5 June 2016; accepted 22 July 2016; published online 22 August 2016)

We have designed and fabricated a structured streak camera photocathode to provide enhanced efficiency for high energy X-rays (1–12 keV). This gold coated photocathode was tested in a Diagnosing Energetic Radiation with streak camera and compared side by side against a conventional flat thin film photocathode. Results show that the measured electron yield enhancement at energies ranging from 1 to 10 keV scales well with predictions, and that the total enhancement can be more than 3×. The spatial resolution of the streak camera does not show degradation in the structured region. We predict that the temporal resolution of the detector will also not be affected as it is currently dominated by the slit width. This demonstration with Au motivates exploration of comparable enhancements with CsI and may revolutionize X-ray streak camera photocathode design. *Published by AIP Publishing.* [<http://dx.doi.org/10.1063/1.4961302>]

## I. OVERVIEW

X-ray diagnostics are an integral part of experiments performed at the National Ignition Facility (NIF).<sup>1</sup> For example, Diagnostic Instrument Manipulator Imaging Streak Camera (DISC)<sup>2</sup> and Streaked Polar Instrumentation for Diagnosing Energetic Radiation (SPIDER)<sup>3</sup> are used as temporal imagers in radiography studies, as streaked X-ray spectrometers for backlighter source characterization, and as timing instruments. Drift tube detectors such as the Dilation X-ray Imager (DIXI)<sup>4,5</sup> are used as 2-D imagers of imploding targets. Until recently, these detectors have been used to collect data in the 1–10 keV range. A new, Advanced Radiographic Capability (ARC)<sup>6</sup> has been introduced to NIF. ARC uses four existing NIF beams to produce short (30 ps currently) pulses with ~1 kJ laser energy each. The new set of short pulse beams will extend the available X-ray energies up to >300 keV. Current diagnostics, especially those that utilize common photocathode materials, suffer from a drastic decrease in quantum efficiency above ~10 keV.<sup>7–10</sup> This reduces the detector efficiency of the NIF detectors and can potentially compromise data quality.

There has been an ongoing effort to identify and test a set of geometrically enhanced photocathodes in order to improve the detector efficiency of current NIF X-ray cameras. During this multi-year project, a photocathode structure prototype was identified,<sup>9</sup> fabricated,<sup>11</sup> and characterized. This work

led to the fabrication and performance test of a full-scale photocathode prototype in SPIDER. The measured signal increase, along with the effects of the full-scale structured photocathode on the streak camera performance, is presented in this manuscript.

## II. EXPERIMENTAL SETUP

A broadband Manson X-ray source<sup>12</sup> was used to characterize the performance of three full-scale structured photocathodes. The source was set to generate Ni K- $\alpha$  lines at ~7.5 keV by adjusting the anode to filament voltage and using a 3  $\mu\text{m}$  thick Ni filter, as shown in Fig. 1. The photocathodes were tested in a fully calibrated SPIDER detector. SPIDER is a multi-record length streak camera system, with a 1.2 times magnification and ~87  $\mu\text{m}$  spatial resolution.<sup>3</sup> Potential changes in spatial resolution were measured by using a spatial resolution mask. The mask was laser cut into a 20  $\mu\text{m}$  thick Ta foil, and the pattern contained a series of 50  $\mu\text{m}$  wide slits evenly spaced 1.5 mm apart. The pattern was placed directly in front of each photocathode and 1 meter away from the X-ray source.

The photocathode design was based on the recessed pyramid structure described in previous publications.<sup>9,11</sup> The photocathode shown in Fig. 2 consisted of two regions, a flat surface and a structured surface. The structures were etched into a Si substrate using a plasma etching system, producing a high aspect ratio structure with 10°–15° wall angles. The Si substrate was back-thinned to 100  $\mu\text{m}$  under both regions, in order to maximize X-ray transmission, i.e., 18% transmission at 7.5 keV. Both regions were coated with a Ti wetting layer

Note: Contributed paper, published as part of the Proceedings of the 21st Topical Conference on High-Temperature Plasma Diagnostics, Madison, Wisconsin, USA, June 2016.

<sup>a)</sup>Author to whom correspondence should be addressed. Electronic mail: opachiyp@nv.doe.gov

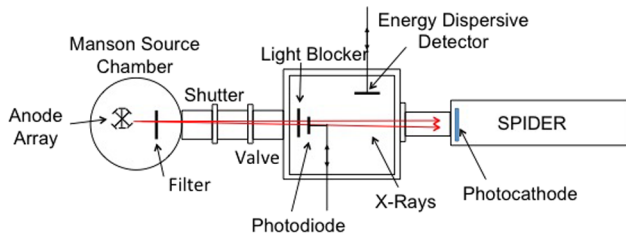


FIG. 1. Experimental setup. The Manson source layout is shown, starting with the vacuum chamber that contains the anode array on the left. The streak camera is placed 1 meter away from the anode source.

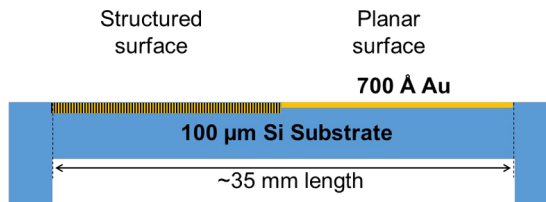


FIG. 2. Cross sectional view of the full-scale photocathode. The side by side flat and structured photocathode regions are shown, and the entire prototype is coated with 700 Å of gold. The Si substrate is back etched to 100 μm thickness.

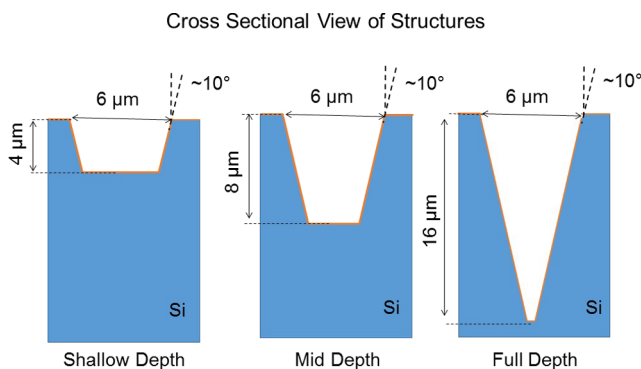


FIG. 3. A cross sectional view of the recessed pyramid structures in the structured surface region of the photocathodes. Examples of the three cathode types are shown: the shallow depth, mid depth, and full depth.

and 700 Å of gold. The prototype cathodes consisted of recessed pyramid structures that were  $6 \times 6 \mu\text{m}$  in width and had three depths 4, 8, and 16 μm, respectively, see Fig. 3. These are referred to as the shallow depth, mid depth, and full depth structures throughout the manuscript. The side by side design was developed to ensure that the two regions are easily comparable within the same exposure.

### III. DISCUSSION AND RESULTS

Two measurements were conducted to identify potential detector performance changes caused by the presence of a structured photocathode surface: an evaluation of the fractional signal increase collected from the structured region and a study of changes in spatial resolution that may have been introduced by the structures.

To characterize improvement in signal level, X-ray images were recorded for each prototype. The recorded side by side signal image of the full depth structure is shown in Fig. 4. The image was background subtracted and flat fielded to take

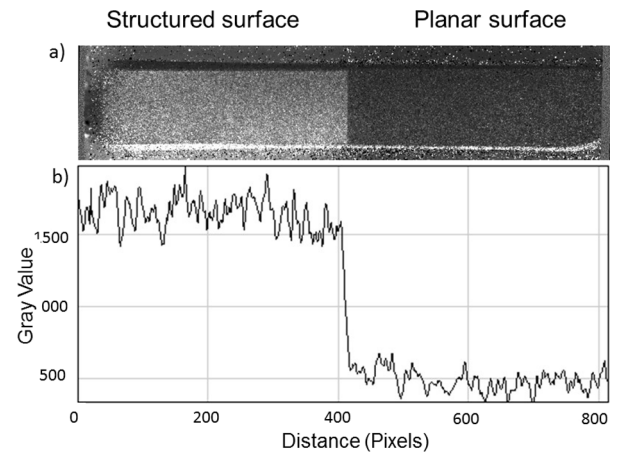


FIG. 4. Structured photocathode test results. The photocathode CCD image is shown in the top panel, and a lineout covering the central 1/4 regions through both the structured and planar cathode areas is shown below.

out non-uniformities introduced by the SPIDER imaging system. Typically background levels were near  $\sim 510$  counts, with the lowest signal of 500 counts above background recorded in the planar cathode region. The bright region seen in Fig. 4 corresponds to that of the full depth recessed pyramid structures. A lineout through the interface is presented below the image, showing an increase in signal of  $\sim 3.5\times$ . An increase in signal between  $2.7\times$  and  $4.5\times$  was expected for this structure; details of the model and calculations are given in our previous publication.<sup>9</sup> In terms of total quantum efficiency, a planar Au photocathode at 7.5 keV emits an average of 0.015<sup>8</sup> electrons per photon; we measure that the structured surfaces in our work increase this number to 0.05. The predicted and measured yield from all three structures is summarized in Table I. The measured fractional increase is defined as the ratio between the signals recorded in the structured region and flat surface region. The increase in yield from the mid depth to the full depth is smaller than predicted; we believe this is potentially caused by differences in the etched wall angles and widths of the two prototypes, an etch that is not fully tapered to a full cone and a decrease in the electric field strength within the full depth cavity that may be trapping emitted electrons. In general, the measured data fall within the predicted yield increase, verifying our model and calculations.

The spatial resolution of SPIDER was measured using a standard planar photocathode and compared with the results from all three prototypes. A single spatial resolution mask was used for all measurements, and the resulting line spread functions (LSF) are shown in Fig. 5. Each LSF was normalized

TABLE I. Summary of measurement results for three structured photocathodes.

Cathode type	Structure dimensions ( $\mu\text{m}$ )	Measured fractional increase	Predicted fractional increase	LSF FWHM ( $\mu\text{m}$ )
Shallow depth	$6 \times 6 \times 4$	$2.3 \pm 0.02$	2.2–2.4	$87 \pm 8$
Mid depth	$6 \times 6 \times 8$	$3.2 \pm 0.04$	2.9–3.5	$88 \pm 10$
Full depth	$6 \times 6 \times 16$	$3.5 \pm 0.01$	2.7–4.5	$85 \pm 14$

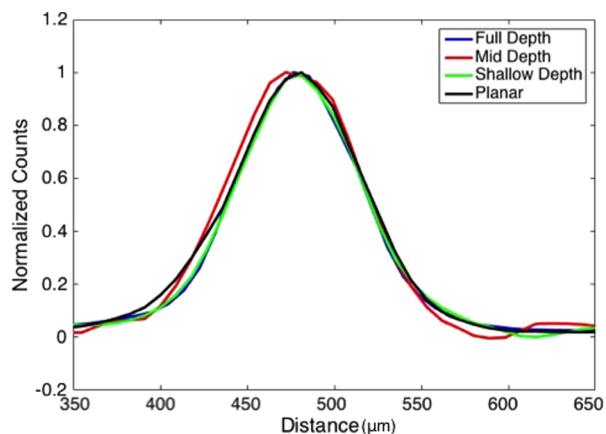


FIG. 5. Measured spatial resolution. Spatial resolution is not affected by the addition of the structured surface. Resolution matches that of the standard cathode for structures of all depths.

to unity and then fitted to a Gaussian function to determine the full width at half maximum (FWHM). The mid depth structure appears to have the widest FWHM; this is typically caused by a slightly wider width of the etched recessed pyramid. For all three structures, no correlation was seen between the LSF width and structure depth, showing that the chosen  $6 \times 6 \mu\text{m}$  width was appropriate and the spatial resolution of the detector is not affected by the introduction of the structured surfaces. The standard spatial resolution at the photocathode was measured to be  $87 \pm 10 \mu\text{m}$ , while the spatial resolution obtained from the structured region ranged from  $85 \mu\text{m}$  to  $88 \mu\text{m}$ . The width varies mostly due to different signal to noise levels. The spatial resolution results are summarized in the last column of Table I.

#### IV. CONCLUSIONS

A geometrically enhanced photocathode has been developed and tested in a NIF streak camera, SPIDER. The results show an increase in yield of up to  $3.5\times$  at  $7.5 \text{ keV}$ . The measured increase in yield falls within the predictions made for this structure. It was also shown that the structured photocathode surface does not affect the spatial resolution of the detector. Temporal resolution measurements should be

performed in the future to ensure that the detector performance remains unchanged. This demonstration with Au motivates exploration of comparable enhancements with CsI and may revolutionize X-ray streak camera photocathode design.

#### ACKNOWLEDGMENTS

This work was done by National Security Technologies, LLC, under Contract No. DE-AC52-06NA25946 with the U.S. Department of Energy and supported by the Site-Directed Research and Development Program, DOE/NV/25946-2838.

- <sup>1</sup>G. H. Miller, E. I. Moses, and C. R. Wuest, *Nucl. Fusion* **44**, S228 (2004).
- <sup>2</sup>Y. P. Opachich, D. H. Kalantar, A. G. MacPhee, J. P. Holder, J. R. Kimbrough, P. M. Bell, D. K. Bradley, B. Hatch, G. Brienza-Larsen, C. Brown, C. G. Brown, D. Browning, M. Charest, E. L. Dewald, M. Griffin, B. Guidry, M. J. Haugh, D. G. Hicks, D. Homoelle, J. J. Lee, A. J. Mackinnon, A. Mead, N. Palmer, B. H. Perfect, J. S. Ross, C. Silbernagel, and O. Landen, *Rev. Sci. Instrum.* **83**, 125105 (2012).
- <sup>3</sup>S. F. Khan, P. M. Bell, D. K. Bradley, S. R. Burns, J. R. Celeste, L. S. Dauffy, M. J. Eckart, M. A. Gerhard, C. Hagmann, D. I. Headley, J. P. Holder, N. Izumi, M. C. Jones, J. W. Kellogg, H. Y. Khater, J. R. Kimbrough, A. G. MacPhee, Y. P. Opachich, N. E. Palmer, R. B. Petre, J. L. Porter, R. T. Shelton, T. L. Thomas, and J. B. Worden, *Proc. SPIE* **8505**, 850505 (2012).
- <sup>4</sup>T. J. Hilsabeck, J. D. Hares, J. D. Kilkenny, P. M. Bell, A. K. L. Dymoke-Bradshaw, J. A. Koch, P. M. Celliers, D. K. Bradley, T. McCarville, M. Pivovarov, R. Soufli, and R. Bionta, *Rev. Sci. Instrum.* **81**, 10E317 (2010).
- <sup>5</sup>S. R. Nagel, T. J. Hilsabeck, P. M. Bell, D. K. Bradley, M. J. Ayers, M. A. Barrios, B. Felker, R. F. Smith, G. W. Collins, O. S. Jones, J. D. Kilkenny, T. Chung, K. Piston, K. S. Raman, B. Sammulu, J. D. Hares, and A. K. L. Dymoke-Bradshaw, *Rev. Sci. Instrum.* **83**, 10E116 (2012).
- <sup>6</sup>J. M. Di Nicola, S. T. Yang, C. D. Boley, J. K. Crane, J. E. Heebner, T. M. Spinka, P. Arnold, C. P. J. Barty, M. W. Bowers, T. S. Budge, K. Christensen, J. W. Dawson, G. Erbert, E. Feigenbaum, G. Guss, C. Haefner, M. R. Hermann, D. Homoelle, J. A. Jarboe, J. K. Lawson, R. Lowe-Webb, K. McCandless, B. McHale, L. J. Pelz, P. P. Pham, M. A. Prantil, M. L. Rehak, M. A. Rever, M. C. Rushford, R. A. Sacks, M. Shaw, D. Smauley, L. K. Smith, R. Speck, G. Tietbohl, P. J. Wegner, and C. Widmayer, *Proc. SPIE* **9345**, 93450I (2015).
- <sup>7</sup>T. Hara, Y. Tanaka, H. Kitamura, and T. Ishikawa, *Rev. Sci. Instrum.* **71**, 3624 (2000).
- <sup>8</sup>B. L. Henke, J. P. Knauer, and K. Premaratne, *J. Appl. Phys.* **52**, 1509 (1981).
- <sup>9</sup>Y. P. Opachich, P. W. Ross, A. G. MacPhee, T. J. Hilsabeck, S. R. Nagel, E. Huffman, P. M. Bell, D. K. Bradley, J. A. Koch, and O. L. Landen, *Rev. Sci. Instrum.* **85**, 11D625 (2014).
- <sup>10</sup>T. Boutboul, A. Akkerman, A. Gibrekhterman, A. Breskin, and R. Chechik, *J. Appl. Phys.* **86**, 5841 (1999).
- <sup>11</sup>Y. P. Opachich, N. Chen, P. M. Bell, D. K. Bradley, J. Feng, A. Gopal, T. J. Hilsabeck, E. Huffman, J. A. Koch, O. Landen, A. MacPhee, S. R. Nagel, and S. Udin, *Proc. SPIE* **9591**, 95910O (2015).
- <sup>12</sup>See <http://www.austinst.com/> for Austin Instruments, Inc.